

A Population of Gamma-Ray Millisecond Pulsars Seen with the Fermi Large Area Telescope

A. A. Abdo,¹ M. Ackermann,² M. Ajello,² W. B. Atwood,³ M. Axelsson,^{4,5} L. Baldini,⁶ J. Ballet,⁷ G. Barbiellini,^{8,9} M. G. Baring,¹⁰ D. Bastieri,^{11,12} B. M. Baughman,¹³ K. Bechtol,² R. Bellazzini,⁶ B. Berenji,² G. F. Bignami,¹⁴ R. D. Blandford,² E. D. Bloom,² E. Bonamente,^{15,16} A. W. Borgland,² J. Bregeon,⁶ A. Brez,⁶ M. Brigida,^{17,18} P. Bruel,¹⁹ T. H. Burnett,²⁰ G. A. Caliandro,^{17,18} R. A. Cameron,² F. Camilo,²¹ P. A. Caraveo,²² P. Carlson,^{4,23} J. M. Casandjian,⁷ C. Cecchi,^{15,16} Ö. Çelik,²⁴ E. Charles,² A. Chekhtman,^{1,25} C. C. Cheung,²⁴ J. Chiang,² S. Ciprini,^{15,16} R. Claus,² I. Cognard,²⁶ J. Cohen-Tanugi,²⁷ L. R. Cominsky,²⁸ J. Conrad,^{4,23,29} R. Corbet,^{24,30} S. Cutini,³¹ C. D. Dermer,¹ G. Desvignes,²⁶ A. de Angelis,³² A. de Luca,¹⁴ F. de Palma,^{17,18} S. W. Digel,² M. Dormody,³ E. do Couto e Silva,² P. S. Drell,² R. Dubois,² D. Dumora,^{33,34} Y. Edmonds,² C. Farnier,²⁷ C. Favuzzi,^{17,18} S. J. Fegan,¹⁹ W. B. Focke,² M. Frailis,³² P. C. C. Freire,³⁵ Y. Fukazawa,³⁶ S. Funk,² P. Fusco,^{17,18} F. Gargano,¹⁸ D. Gasparrini,³¹ N. Gehrels,^{24,37} S. Germani,^{15,16} B. Giebels,¹⁹ N. Giglietto,^{17,18} F. Giordano,^{17,18} T. Glanzman,² G. Godfrey,² I. A. Grenier,² M. H. Grondin,^{33,34} J. E. Grove,¹ L. Guillemot,^{33,34*} S. Guiriec,³⁸ Y. Hanabata,³⁶ A. K. Harding,²⁴ M. Hayashida,² E. Hays,²⁴ G. Hobbs,³⁹ R. E. Hughes,¹³ G. Jóhannesson,² A. S. Johnson,² R. P. Johnson,³ T. J. Johnson,^{24,37*} W. N. Johnson,¹ S. Johnston,³⁹ T. Kamae,² H. Katagiri,³⁶ J. Kataoka,⁴⁰ N. Kawai,^{41,42} M. Kerr,^{20*} J. Knödseder,⁴³ M. L. Kocian,² M. Kramer,⁴⁴ M. Kuss,⁶ J. Lande,² L. Latronico,⁶ M. Lemoine-Goumard,^{33,34} F. Longo,^{8,9} F. Loparco,^{17,18} B. Lott,^{33,34} M. N. Lovellette,¹ P. Lubrano,^{15,16} G. M. Madejski,² A. Makeev,^{1,25} R. N. Manchester,³⁹ M. Marelli,²² M. N. Mazziotta,¹⁸ W. McConville,^{24,37} J. E. McEnery,²⁴ M. A. McLaughlin,⁴⁵ C. Meurer,^{4,29} P. F. Michelson,² W. Mitthumsiri,² T. Mizuno,³⁶ A. A. Moiseev,^{37,46} C. Monte,^{17,18} M. E. Monzani,² A. Morselli,⁴⁷ I. V. Moskalenko,² S. Murgia,² P. L. Nolan,² J. P. Norris,⁴⁸ E. Nuss,²⁷ T. Ohsugi,³⁶ N. Omodei,⁶ E. Orlando,⁴⁹ J. F. Ormes,⁴⁸ D. Paneque,² J. H. Panetta,² D. Parent,^{33,34} V. Pelassa,²⁷ M. Pepe,^{15,16} M. Pesce-Rollins,⁶ F. Piron,²⁷ T. A. Porter,³ S. Rainò,^{17,18} R. Rando,^{11,12} S. M. Ransom,⁵⁰ P. S. Ray,¹ M. Razzano,⁶ N. Rea,^{51,52} A. Reimer,^{2,53} O. Reimer,^{2,53} T. Reposeur,^{33,34} S. Ritz,²⁴ L. S. Rochester,² A. Y. Rodriguez,⁵² R. W. Romani,² M. Roth,²⁰ F. Ryde,^{4,23} H. F. W. Sadrozinski,³ D. Sanchez,¹⁹ A. Sander,¹³ P. M. Saz Parkinson,³ J. D. Scargle,⁵⁴ T. L. Schalk,³ C. Sgrò,⁶ E. J. Siskind,⁵⁵ D. A. Smith,^{33,34*} P. D. Smith,¹³ G. Spandre,⁶ P. Spinelli,^{17,18} B. W. Stappers,⁴⁴ J. L. Starck,⁷ E. Striani,^{47,56} M. S. Strickman,¹ D. J. Suson,⁵⁷ H. Tajima,² H. Takahashi,³⁶ T. Tanaka,² J. B. Thayer,² J. G. Thayer,² G. Theureau,²⁶ D. J. Thompson,²⁴ S. E. Thorsett,³ L. Tibaldo,^{11,12} D. F. Torres,^{52,58} G. Tosti,^{15,16} A. Tramacere,^{2,59} Y. Uchiyama,² T. L. Usher,² A. Van Etten,² V. Vasileiou,^{30,46} C. Venter,^{24,60} N. Vilchez,⁴³ V. Vitale,^{47,56} A. P. Waite,² E. Wallace,²⁰ P. Wang,² K. Watters,² N. Webb,⁴³ P. Weltevrede,³⁹ B. L. Winer,¹³ K. S. Wood,¹ T. Ylinen,^{4,23,61} M. Ziegler³

¹Space Science Division, Naval Research Laboratory, Washington, DC 20375, USA. ²W. W. Hansen Experimental Physics Laboratory, Kavli Institute for Particle Astrophysics and Cosmology, Department of Physics and SLAC National Accelerator Laboratory, Stanford University, Stanford, CA 94305, USA. ³Santa Cruz Institute for Particle Physics, Department of Physics and Department of Astronomy and Astrophysics, University of California, Santa Cruz, CA 95064, USA. ⁴Oskar Klein Centre for Cosmo Particle Physics, AlbaNova, SE106 91 Stockholm, Sweden. ⁵Department of Astronomy, Stockholm University, SE106 91 Stockholm, Sweden. ⁶Istituto Nazionale di Fisica Nucleare, Sezione di Pisa, I56127 Pisa, Italy. ⁷Laboratoire AIM, CEA/IRFU/CNRS/Université Paris Diderot, Service d'Astrophysique, CEA Saclay, 91191 Gif sur Yvette, France. ⁸Istituto Nazionale di Fisica Nucleare, Sezione di Trieste, I34127 Trieste, Italy. ⁹Dipartimento di Fisica, Università di Trieste, I34127 Trieste, Italy. ¹⁰Department of Physics and Astronomy, Rice University, Houston, TX 77251, USA. ¹¹Istituto Nazionale di Fisica Nucleare, Sezione di Padova, I35131 Padova, Italy. ¹²Dipartimento di Fisica "G. Galilei," Università di Padova, I35131 Padova, Italy. ¹³Department of Physics, Center for Cosmology and AstroParticle Physics, Ohio State University, Columbus, OH 43210, USA. ¹⁴Istituto Universitario di Studi Superiori (IUSS), I27100 Pavia, Italy. ¹⁵Istituto Nazionale di Fisica Nucleare, Sezione di Perugia, I06123 Perugia, Italy. ¹⁶Dipartimento di Fisica, Università degli Studi di Perugia, I06123 Perugia, Italy. ¹⁷Dipartimento di Fisica "M. Merlin" dell'Università e del Politecnico di Bari, I70126 Bari, Italy. ¹⁸Istituto Nazionale di Fisica Nucleare, Sezione di Bari, I70126 Bari, Italy. ¹⁹Laboratoire Leprince-Ringuet, École Polytechnique, CNRS/IN2P3, Palaiseau, France. ²⁰Department of Physics, University of Washington, Seattle, WA 98195, USA. ²¹Columbia Astrophysics Laboratory, Columbia University, New York, NY 10027, USA. ²²INAF Istituto di Astrofisica Spaziale e Fisica Cosmica, I20133 Milano, Italy. ²³Department of Physics, Royal Institute of Technology (KTH), AlbaNova, SE106 91 Stockholm, Sweden. ²⁴NASA Goddard Space Flight Center, Greenbelt, MD 20771, USA. ²⁵George Mason University, Fairfax, VA 22030, USA. ²⁶Laboratoire de Physique et Chimie de l'Environnement, LPCE UMR 6115 CNRS, F45071 Orléans Cedex 02, and Station de Radioastronomie de Nançay, Observatoire de Paris, CNRS/INSU, F18330 Nançay, France. ²⁷Laboratoire de Physique Théorique et Astroparticules, Université Montpellier 2, CNRS/IN2P3, Montpellier, France. ²⁸Department of Physics and Astronomy, Sonoma State University, Rohnert Park, CA 94928, USA. ²⁹Department of Physics, Stockholm University, AlbaNova, SE106 91 Stockholm, Sweden. ³⁰University of Maryland, Baltimore County, Baltimore, MD 21250, USA. ³¹Agenzia Spaziale Italiana (ASI) Science Data Center, I00044 Frascati (Roma), Italy. ³²Dipartimento di Fisica, Università di Udine and Istituto Nazionale di Fisica Nucleare, Sezione di Trieste, Gruppo Collegato di Udine, I33100 Udine, Italy. ³³CNRS/IN2P3, Centre d'Études Nucléaires Bordeaux Gradignan, UMR 5797, 33175 Gradignan, France. ³⁴Université de Bordeaux, Centre d'Études Nucléaires Bordeaux Gradignan, UMR 5797, 33175 Gradignan, France. ³⁵Arecibo Observatory, Arecibo, PR 00612, USA. ³⁶Department of Physical Sciences, Hiroshima University, Higashi Hiroshima, Hiroshima 7398526, Japan. ³⁷University of Maryland, College Park, MD 20742, USA. ³⁸University of Alabama, Huntsville, AL 35899, USA. ³⁹Australia Telescope National Facility, CSIRO, Epping, NSW 1710, Australia. ⁴⁰Waseda University, 1104 Totsukamachi, Shinjuku, Tokyo 1698050, Japan. ⁴¹Cosmic Radiation Laboratory, Institute of Physical and Chemical Research (RIKEN), Wako, Saitama 3510198, Japan. ⁴²Department of Physics, Tokyo Institute of Technology, Meguro City, Tokyo 1528551, Japan. ⁴³Centre d'Étude Spatiale des Rayonnements, CNRS/UPS, BP 44346, F30128 Toulouse Cedex 4, France. ⁴⁴Jodrell Bank Centre for Astrophysics, School of Physics and Astronomy, University of Manchester, Manchester M13 9PL, UK. ⁴⁵Department of Physics, West Virginia University, Morgantown, WV 26506, USA. ⁴⁶Center for Research and Exploration in Space Science and Technology, NASA Goddard Space Flight Center, Greenbelt, MD 20771, USA. ⁴⁷Istituto Nazionale di Fisica Nucleare, Sezione di Roma "Tor Vergata," I00133 Roma, Italy. ⁴⁸Department of Physics and Astronomy, University of Denver, Denver, CO 80208, USA. ⁴⁹Max-Planck-Institut für Extraterrestrische Physik, 85748 Garching, Germany. ⁵⁰National Radio Astronomy Observatory (NRAO), Charlottesville, VA 22903 USA. ⁵¹Sterrenkundig Instituut "Anton Pannekoek," 1098 SJ Amsterdam, Netherlands. ⁵²Institut de Ciències de l'Espai (IEECCSIC), Campus UAB, 08193 Barcelona, Spain. ⁵³Institut für Astro und Teilchenphysik, Leopold-Franzens-Universität Innsbruck, A6020 Innsbruck, Austria. ⁵⁴Space Sciences Division, NASA Ames Research Center, Moffett Field, CA 94035, USA. ⁵⁵NYCB RealTime Computing Inc., Lattingtown, NY 11560, USA. ⁵⁶Dipartimento di Fisica, Università di Roma "Tor Vergata," I00133 Roma, Italy. ⁵⁷Department of Chemistry and Physics, Purdue University Calumet, Hammond, IN 46323, USA. ⁵⁸Institució Catalana de Recerca i Estudis Avançats, Barcelona, Spain. ⁵⁹Consorzio Interuniversitario per la Fisica Spaziale (CIFS), I10133 Torino, Italy. ⁶⁰Unit for Space Physics, NorthWest University, Potchefstroom Campus, Private Bag X6001, Potchefstroom 2520, South Africa. ⁶¹School of Pure and Applied Natural Sciences, University of Kalmar, SE391 82 Kalmar, Sweden.

*To whom correspondence should be addressed. E-mail: guillemo@cenbg.in2p3.fr (L.G.); tyrel.j.johnson@nasa.gov (T.J.J.); kerrm@u.washington.edu (M.K.); smith@cenbg.in2p3.fr (D.A.S.)

Pulsars are born with sub-second spin periods and slow by electromagnetic braking for several tens of millions of years, when detectable radiation ceases. A second life can occur for neutron stars in binary systems. They can acquire mass and angular momentum from their companions, to be spun up to millisecond periods and begin radiating again. We searched Fermi Large Area Telescope data for pulsations from all known millisecond pulsars (MSPs) outside of globular clusters using rotation parameters from radio telescopes. Strong gamma-ray pulsations were detected for eight MSPs. The gamma-ray pulse profiles and spectral properties resemble those of young gamma-ray pulsars. The basic emission mechanism seems to be the same for MSPs and young pulsars, with the emission originating in regions far from the neutron star surface.

It took 15 years after the discovery of pulsars before instrumental and computing advances enabled the first radio detections of neutron stars with millisecond spin periods (1). Similarly, 17 years after the launch of the Compton Gamma-Ray Observatory (CGRO), the Large Area Telescope (LAT) on the Fermi Gamma-ray Space Telescope, formerly GLAST, is now revealing new classes of GeV gamma-ray pulsars. Here we report LAT detections of pulsed gamma rays from eight Galactic millisecond pulsars (MSPs), confirming the marginal detection of PSR J0218+4232 made using the EGRET detector on CGRO (2), as well as the first MSP seen with the LAT, PSR J0030+0451 (3). A companion article describes the discovery of many young pulsars based on their gamma-ray emission alone (4). In addition, the LAT has detected about 20 young, radio-loud pulsars (5–7). The AGILE collaboration has recently detected pulsed gamma-ray emission from an MSP in the globular cluster M28 (8).

The Fermi LAT measurements of pulsars in all three of these categories will clarify how neutron stars accelerate the charged particles that radiate at gamma-ray and lower energies. Observed pulse profiles depend on the beam shapes and how they sweep across the Earth; comparison of the radio, X-ray, and gamma-ray profiles constrain models of beam formation in pulsar magnetospheres. For gamma-ray pulsars, the high-energy emission dominates the power of the observed electromagnetic radiation (9). Consequently, gamma rays provide a probe of these cosmic accelerators. Millisecond pulsars shine for billions of years longer than normal pulsars. We now know that they can radiate brightly in gamma rays.

The LAT images the entire sky every 3 hours at photon energies from 20 MeV to >300 GeV (10). Incident gamma rays convert to e-e+ pairs in tungsten foils, leaving tracks in single-sided silicon strip detectors that provide the photon direction. A hodoscopic CsI calorimeter samples the photon

energy, and charged particles are rejected using information from a segmented scintillator array.

Millisecond pulsars (MSPs) form a distinct class, with small spin periods ($P < 30$ ms) and miniscule braking rates ($\dot{P} < 10^{-17}$). Most are in binary systems. The idea that they have been spun-up by the torque due to accretion of mass from their companions (11) is supported by the recent observations reported in (12). MSPs are 10^8 to 10^{10} years old, compared to ages of 10^3 to 10^5 years for the young gamma-ray pulsars. Their surface magnetic fields are a factor of 10^4 weaker than when the neutron star first formed. However, both the rate of rotational kinetic energy loss, $\dot{E} = 4\pi^2 I \dot{P} / P^3$ (on the assumptions of dipole magnetic fields and a neutron star moment of inertia $I = 10^{45}$ g cm²), and the magnetic field at the light cylinder,

$$B_{\text{LC}} = 4\pi^2 \left(3I\dot{P} / 2c^3 P^5 \right)^{1/2},$$

are comparable to those of newly formed pulsars (13). On the basis of theoretical models of gamma-ray emission from MSPs, it was predicted that Fermi would detect roughly 10 pulsed detections in 1 year (14, 15).

The ATNF pulsar database (V1.35) (16) lists 1794 spin-powered pulsars, of which 168 have $P < 30$ ms and $\dot{P} < 10^{-17}$. Of these, 96 are in globular clusters (17). In this article we consider the 72 remaining field MSPs. A radio and X-ray pulsar timing campaign provided rotation ephemerides for Fermi (18). MSP timing solutions were obtained from the Nançay radio telescope (19), Parkes radio telescope (20), Green Bank Telescope (21), Jodrell Bank Lovell Telescope (22), Arecibo radio telescope (23) and Westerbork radio telescope (24). For six of the field MSPs, we used non-contemporaneous ephemerides from the ATNF database. The timing parameters used in this work will be made available on the servers of the Fermi Science Support Center (25).

For the gamma-ray timing analysis, we used LAT data acquired from 30 June 2008 to 15 March 2009, selecting events with energy > 0.1 GeV that pass the Diffuse gamma-ray selection cuts (10). For pulsars with Galactic latitude $|b| > 10^\circ$ we selected events within 1° of the radio position, reduced to 0.5° for $|b| < 10^\circ$, due to the bright gamma-ray background in the Galactic plane caused by cosmic rays interacting with the interstellar medium. LAT photon arrival times are recorded with an accuracy relative to UTC better than 1 μ s (26).

Following this analysis, eight MSPs showed strong gamma-ray pulsations with H-test (27) values > 25 (Fig. 1 and Table 1). Three are associated with EGRET sources: PSRs J0030+0451, J0218+4232, and J1614-2230. The latter

was discovered in a radio search of unidentified EGRET sources (28). All of the detected pulsars had contemporaneous radio ephemerides with weighted rms timing residuals of 10 μ s or less. For all eight MSPs, uncertainties in the dispersion measure lead to uncertainties of less than 0.005 rotations in the extrapolation of the radio pulse arrival times to infinite frequency, negligible for the gamma-ray light-curve bin widths imposed by the photon counts. Analyses for PSRs J0218+4232, J0613-0200, J1614-2240, J1744-1134, and J2144-3358 using ephemerides from different observatories confirmed the absolute phase alignment.

We also searched for steady point-source emission at the locations of the 72 field MSPs. For 13 locations, including those of the eight pulsed detections, emission exceeded the diffuse gamma-ray background by at least 5σ . For the five sources for which only steady emission was seen, the 95% confidence level radii contain no other candidates besides PSRs J0034-0534, J0610-2100, J1600-3053, J1939+2134, and J1959+2048.

We used the spectral likelihood methods described in (29) (SOM). To reduce the background from cosmic-ray interactions in the upper atmosphere, we required photon zenith angles to be less than 105° and excluded time periods when the Earth's limb came within 28° of the source. Because of uncertainties in the instrument response, we rejected events with energies below 0.2 GeV. We modeled the gamma-ray spectra with an exponentially cutoff power-law of the form

$$N_0 E^{-\Gamma} \exp\left[-(E/E_c)\right],$$

where N_0 is a normalization factor (Table 1). The cutoff energies range from 1 GeV to almost 4 GeV (neglecting the J0218+4232 cutoff which has a large error) and the spectra are hard ($\Gamma < 2$). Overall, the MSP spectral shapes resemble those of young pulsars.

We converted the integral energy fluxes to luminosities using $L_\gamma = 4\pi h d^2$, where d is the pulsar distance. This corresponds to a flux correction factor $f_\Omega = 1$, appropriate for a fan-like beam as given by outer magnetosphere emission models (30). Six of the pulsars are close and have parallax distance measurements (31–33), although, in some cases, uncertainties are large. The distances to PSR J0218+4232 and PSR J1614-2230 are based on the dispersion measures and the NE2001 Galactic electron density model (34). MSPs have low intrinsic \dot{P} values and are relatively close, hence the kinematic Shklovskii contribution (35) $\dot{P}_s = \mu^2 d / cP$, where μ is the proper motion, is significant. \dot{P}_s is subtracted

from the observed \dot{P} before computing the spin-down power \dot{E} and the corresponding gamma-ray efficiency $\eta = L_\gamma / \dot{E}$ (Table 1). Uncertainties in \dot{E} are generally a few percent or less, except for PSRs J1614-2230 and J2124-3358 where they are larger (60% and 32% respectively) because the large uncertainty in the distance leads to a correspondingly large uncertainty in \dot{P}_s . Uncertainties in η are much larger because $L_\gamma \sim d^2$ and hence the effect of the distance uncertainty is doubled. The high, albeit uncertain, efficiency for PSR J1614-2230 indicates that the distance is over-estimated. Reducing the distance would both reduce the Shklovskii correction, thereby increasing \dot{E} , and decrease L_γ . Other possible systematic uncertainties in the \dot{E} and η values come from the neutron-star moment of inertia which is assumed to be 10^{45} g cm². Measured values of neutron-star masses cover a range from about 1.25 to 1.75 Solar masses (36, 37) and the estimated moments of inertia vary correspondingly (38). Also, the flux correction factor f_Ω may differ significantly from the assumed value of one (30).

Five of the eight gamma-ray MSPs are in binary systems. An eclipsing orbit, or interactions with the stellar wind of the companion, could affect the gamma-ray flux. We searched for flux variability at their orbital periods but found none exceeding 25% of the flux.

The observed MSP gamma-ray profiles and their relation to the radio profiles are similar to those observed for young pulsars. For PSRs J0030+0451 and J1614-2230, the double-peaked profiles with separation $\Delta \sim 0.45$ and first-peak lag $\delta \sim 0.15$ are almost identical to observed profiles for most young pulsars (5–7, 29). A higher proportion of MSPs have a dominant single gamma-ray peak at $\delta \sim 0.5$, but the young pulsar PSR J2229+6114 has a similar pulse profile. For both MSPs and young pulsars the gamma-ray peaks, single or multiple, are centered on phases 0.3 to 0.4 relative to the radio peak. MSP radio profiles tend to be complex with many components, and in these cases it can be difficult to identify the relevant radio phase. Also, the statistics of the gamma-ray profiles are currently relatively poor.

All detected millisecond and normal gamma-ray pulsars lie above a common threshold of about 5×10^{33} erg s⁻¹ kpc⁻², another similarity between these two classes (Fig. 2). Pulsars undetected in gamma rays of both classes lie above this threshold, possibly because: distance estimates may be in error for individual pulsars; the gamma-ray emission beam (or at least strong parts of it) may not sweep across the Earth; neutron-star moments of inertia may be less than the assumed 10^{45} g cm² for some pulsars, so that a given \dot{P} corresponds to a smaller \dot{E} .

Polar cap (PC) MSP models, where the bulk of the emission originates near the surface of the neutron star, predict that the pulsed gamma rays are roughly aligned with the magnetic poles (39). In outer gap (OG) (40) and slot gap (SG) (41) models, the bulk of the emission originates in the outer magnetosphere in narrow gaps along the last open field lines, forming wide fan beams that are not aligned with the magnetic poles. In the MSP gamma-ray light curves in Fig. 1, we see that although some of the gamma-ray peaks are aligned with the radio peaks that are thought to be aligned with the magnetic poles, most are not. This favors the outer magnetosphere model geometry.

The similarities of the gamma-ray pulse profiles, the \dot{E} dependence, and the spectral properties strongly suggest that the same basic emission mechanism is operating in both classes. Magnetic field strengths at the neutron-star surface, derived assuming dipole fields, differ by four orders of magnitude between MSPs and young pulsars. On the other hand, B_{LC} is comparable for both. Fermi data for young pulsars (5–7, 29) favor outer-magnetosphere emission models over models where the emission comes from close to the polar cap.

The MSP models (39–41) assume curvature radiation from electrons whose energies arise from a balance between acceleration by the pulsar electric field and the curvature radiation loss in a dipole magnetic field. The cutoff energy thus directly measures the accelerating electric field. The observed values in the range 1 – 4 GeV indicate that the emission is not taking place near the surface, where the electric field is stronger and the cutoff energies for MSPs would be closer to 10 – 50 GeV or even higher (42), but at some altitude above the neutron star surface.

For current SG and OG models, only MSPs with the highest spin-down power have a high enough electric potential for electron-positron pair production. Most of the MSPs detected by Fermi are below this threshold. Thus, some revision of the outer-magnetosphere models is needed. Surface magnetic fields may be stronger than assumed, maybe because of magnetic multipoles or more compact neutron stars. Alternatively, maybe the magnetic field at the light cylinder plays a greater role in particle acceleration than has been assumed.

References and Notes

1. D. C. Backer, S. R. Kulkarni, C. Heiles, M. M. Davis, W. M. Goss, *Nature* **300**, 615 (1982).
2. L. Kuiper *et al.*, *Astron. Astrophys.* **359**, 615 (2000).
3. A. A. Abdo *et al.*, *Astrophys. J.* **699**, 1171 (2009).
4. A. A. Abdo *et al.*, *Science* **2** July 2009 (10.1126/science.1175558).
5. A. A. Abdo *et al.* (Fermi LAT Collaboration), *Astrophys. J.* **695**, L72 (2009).
6. A. A. Abdo *et al.* (Fermi LAT Collaboration and Fermi Pulsar Timing Consortium), <http://arxiv.org/abs/0905.4400> (2009).
7. A. A. Abdo *et al.*, *Astrophys. J.* **699**, L102 (2009).
8. A. Pellizzoni *et al.* (Agile Collaboration), *Astrophys. J.* **695**, L115 (2009).
9. D. J. Thompson *et al.*, *Astrophys. J.* **516**, 297 (1999).
10. W. B. Atwood *et al.*, *Astrophys. J.* **697**, 1071 (2009).
11. M. A. Alpar, A. F. Cheng, M. A. Ruderman, J. Shaham, *Nature* **300**, 728 (1982).
12. A. M. Archibald *et al.*, *Science* **324**, 1411 (2009).
13. D. R. Lorimer, M. Kramer, *Handbook of Pulsar Astronomy* (Cambridge Univ. Press, Cambridge, 2004).
14. L. Zhang, J. Fang, S. B. Chen, *Astrophys. J.* **666**, 1165 (2007).
15. S. A. Story, P. L. Gonthier, A. K. Harding, *Astrophys. J.* **671**, 713 (2007).
16. R. N. Manchester, G. B. Hobbs, A. Teoh, M. Hobbs, *Astrophys. J.* **129**, 1993 (2005). The ATNF Pulsar Catalogue is available at www.atnf.csiro.au/research/pulsar/psrcat.
17. F. Camilo, F. A. Rasio, *ASP Conf. Ser.* **328**, 147 (2005).
18. D. A. Smith *et al.*, *Astron. Astrophys.* **492**, 923 (2008).
19. G. Theureau *et al.*, *Astron. Astrophys.* **430**, 373 (2005).
20. R. N. Manchester, *AIP Conf. Ser.* **983**, 584 (2008).
21. D. L. Kaplan *et al.*, *Publ. Astron. Soc. Pac.* **117**, 643 (2005).
22. G. Hobbs, A. G. Lyne, M. Kramer, C. E. Martin, C. Jordan, *Mon. Not. R. Astron. Soc.* **353**, 1311 (2004).
23. A. Dowd, W. Sisk, J. Hagen, *ASP Conf. Ser.* **202**, 275 (2000).
24. J. L. L. Voûte *et al.*, *Astron. Astrophys.* **385**, 733 (2002).
25. Fermi Science Support Center (<http://fermi.gsfc.nasa.gov/ssc>).
26. Fermi LAT Collaboration, <http://arxiv.org/abs/0904.2226> (2009).
27. O. C. de Jager, B. C. Raubenheimer, J. W. H. Swanepoel, *Astron. Astrophys.* **221**, 180 (1989).
28. F. Crawford *et al.*, *Astrophys. J.* **652**, 1499 (2006).
29. A. A. Abdo *et al.* (Fermi LAT Collaboration), *Astrophys. J.* **696**, 1084 (2009).
30. K. P. Watters, R. W. Romani, P. Weltevrede, S. Johnston, *Astrophys. J.* **695**, 1289 (2009).
31. A. N. Lommen *et al.*, *Astrophys. J.* **545**, 1007 (2000).
32. A. T. Deller, J. P. W. Verbiest, S. J. Tingay, M. Bailes, *Astrophys. J.* **685**, 67 (2008).
33. A. W. Hotan, M. Bailes, S. M. Ord, *Mon. Not. R. Astron. Soc.* **369**, 1502 (2006).
34. J. M. Cordes, T. J. W. Lazio, <http://arxiv.org/abs/astro-ph/0207156> (2002).
35. I. S. Shklovskii, *Sov. Astron.* **13**, 562 (1970).
36. M. Kramer *et al.*, *Science* **314**, 97 (2006).
37. J. P. W. Verbiest *et al.*, *Astrophys. J.* **679**, 675 (2008).
38. J. M. Lattimer, M. Prakash, *Science* **304**, 536 (2004).
39. A. K. Harding, V. V. Usov, A. G. Muslimov, *Astrophys. J.* **622**, 531 (2005).
40. L. Zhang, K. S. Cheng, *Astron. Astrophys.* **398**, 639 (2003).
41. A. G. Muslimov, A. K. Harding, *Astrophys. J.* **617**, 471 (2004).
42. T. Bulik, B. Rudak, J. Dyks, *Mon. Not. R. Astron. Soc.* **317**, 97 (2000).

43. A. A. Abdo *et al.*, *Astrophys. J. Suppl. Ser.* **183**, 46 (2009).
44. The Fermi LAT Collaboration acknowledges support from a number of agencies and institutes for both development and the operation of the LAT as well as scientific data analysis. These include NASA and DOE in the United States, CEA/Irfu and IN2P3/CNRS in France, ASI and INFN in Italy, MEXT, KEK, and JAXA in Japan, and the K.A. Wallenberg Foundation, the Swedish Research Council and the National Space Board in Sweden. Additional support from INAF in Italy for science analysis during the operations phase is also gratefully acknowledged. The Parkes telescope is funded by the Commonwealth Government and is managed by CSIRO. The GBT is operated by the NRAO, a facility of the NSF operated under cooperative agreement by Associated Universities, Inc. The Arecibo Observatory is part of the NAIC, operated by Cornell University under a cooperative agreement with the NSF. The NRT is operated by the Paris Observatory, associated with the French CNRS. The Lovell Telescope is owned and operated by the University of Manchester with support from the STFC of the UK. The WSRT is operated by ASTRON in the Netherlands. A.A.A. is a National Research Council Research Associate. J. Conrad is a Royal Swedish Academy of Sciences Research Fellow, funded by a grant from the K. A. Wallenberg Foundation.

contemporaneous rotation parameters are unavailable are shown as squares. Undetected MSPs are indicated by open circles, and small dots show undetected normal pulsars. The young radio-loud gamma-ray pulsars are the seven CGRO detections (9), and recent Fermi detections (7, 43).

Supporting Online Material

www.sciencemag.org/cgi/content/full/1176113/DC1

SOM Text

References

11 May 2009; accepted 24 June 2009

Published online 2 July 2009; 10.1126/science.1176113

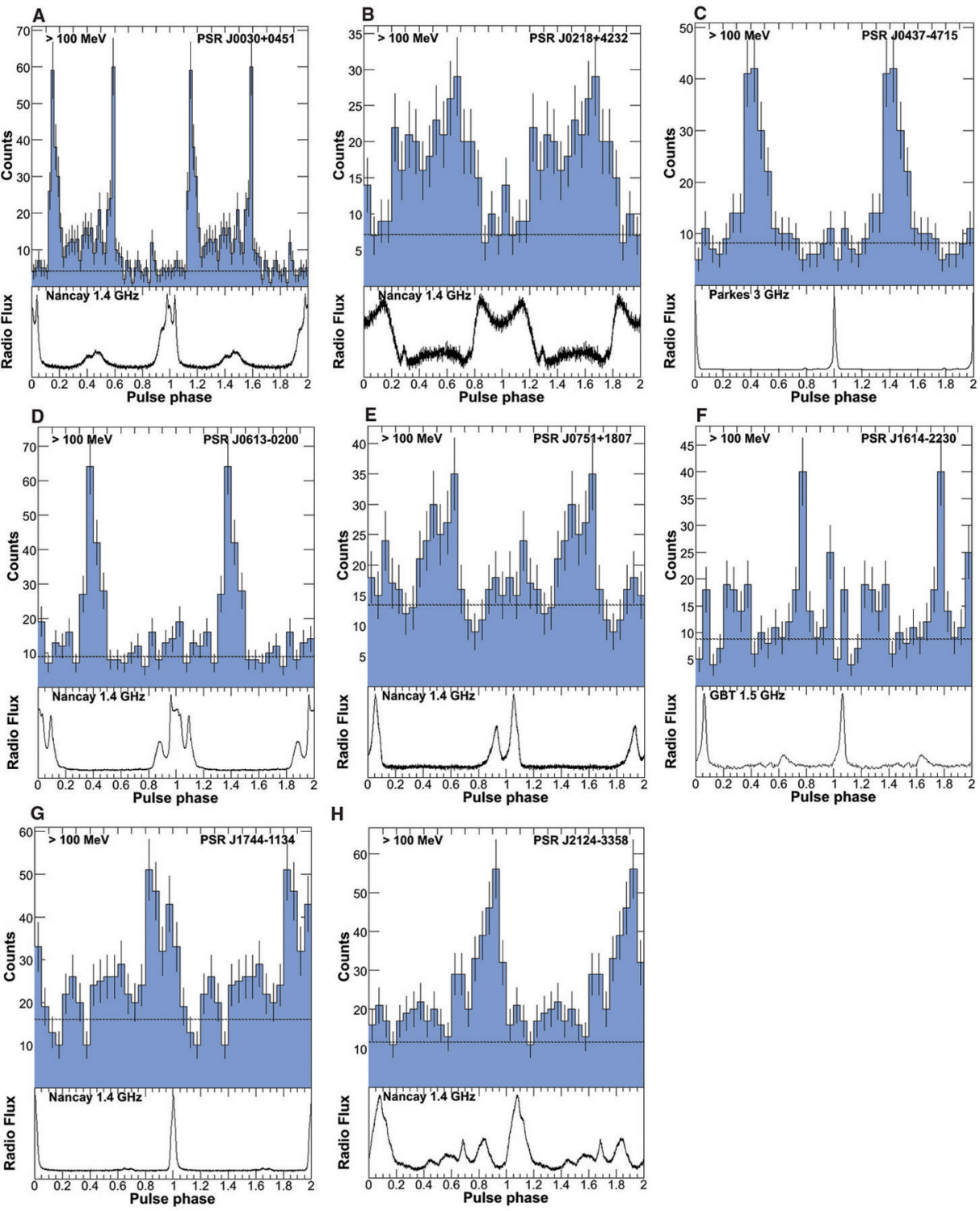
Include this information when citing this paper.

Fig. 1. (A to H) Gamma-ray and radio pulse profiles for the eight millisecond pulsars detected by Fermi. Two rotations are shown and each bin is 0.05 in phase, except for PSR J0030+0451 where each bin is 0.02 wide. Gamma-ray photons are selected by energy above 0.1 GeV and according to the angular cuts discussed in the text, except for J0218+4232 and J1614-2230 for which a 0.5° cut was used because the proximity of the blazar 3C66A for the former and the hard spectrum for the latter. The horizontal dashed lines show the background level estimated from a surrounding ring. The bottom panels show the radio profiles phased relative to the gamma-ray pulses as emitted from the pulsar.

Fig. 2. Spin-down power \dot{E} normalized to the distance squared versus the rotational period for pulsars outside of globular clusters. Where proper motions are available, the \dot{E} values have been corrected for the Shklovskii effect (see text). The eight MSPs reported in this paper are indicated by solid dots, as are young, radio-loud gamma-ray pulsars. The five MSPs likely associated with the non-pulsed point-source detections are indicated by triangles. MSPs for which

Table 1. Properties of the millisecond pulsars detected by Fermi. For each pulsar we give the Galactic longitude and latitude (l, b), the rotational period P , the distance d and the spin-down power \dot{E} . Pulsars marked with a (b) belong to binary systems. The distances come from parallax measurements except for the values marked by an asterisk, which are based on the dispersion measure. The \dot{E} values have been computed using period derivatives corrected for the Shklovskii effect (35). The δ parameter gives the phase offset between the maximum of the radio emission and that of the nearest gamma-ray peak, and Δ is the peak separation for two-peaked gamma-ray profiles. The integral photon and energy fluxes over 0.1 GeV are given, as well as the spectral indices, the exponential cutoff energies, and the gamma-ray emission efficiencies. The systematic uncertainties stemming from the instrument response and the diffuse background are $(-0.1; +0.3)$ for Γ , $(-10\%; +20\%)$ for E_c , $(-10\%; +30\%)$ for the photon flux, and $(-10\%; +20\%)$ for the energy flux.

Pulsar name	l, b	P (ms)	Distance d (pc)	Log \dot{E} (erg/s)	δ	Δ	Photon flux >0.1 GeV (10^{-8} ph $\text{cm}^{-2} \text{s}^{-1}$)	Energy flux >0.1 GeV (10^{-11} erg $\text{cm}^{-2} \text{s}^{-1}$)	Spectral index	Exponential cutoff energy (GeV)	Efficiency η (%)
J0030+0451	113.1°, -57.6°	4.865	300 ± 90	33.54	0.16	0.45	5.5 ± 0.7	4.9 ± 0.3	1.3 ± 0.2	1.9 ± 0.4	15 ± 9
J0218+4232 (b)	139.5°, -17.5°	2.323	2700 ± 600*	35.39	0.50	—	5.6 ± 1.3	3.5 ± 0.5	2.0 ± 0.2	7 ± 4	13 ± 6
J0437-4715 (b)	253.4°, -42.0°	5.757	156 ± 2	33.46	0.45	—	4.4 ± 1.0	1.9 ± 0.3	2.1 ± 0.3	2.1 ± 1.1	1.9 ± 0.3
J0613-0200 (b)	210.4°, -9.3°	3.061	480 ± 140	34.10	0.42	—	3.1 ± 0.7	3.1 ± 0.3	1.4 ± 0.2	2.9 ± 0.7	7 ± 4
J0751+1807 (b)	202.7°, 21.1°	3.479	620 ± 310	33.85	0.42	—	2.0 ± 0.7	1.7 ± 0.2	1.6 ± 0.2	3.4 ± 1.2	11 ± 11
J1614-2230 (b)	352.5°, 20.3°	3.151	1300 ± 250*	33.7	0.20	0.48	2.3 ± 2.1	2.5 ± 0.8	1.0 ± 0.3	1.2 ± 0.5	100 ± 80
J1744-1134	14.8°, 9.2°	4.075	470 ± 90	33.60	0.85	—	7.1 ± 1.4	4.0 ± 1.0	1.5 ± 0.2	1.1 ± 0.2	27 ± 12
J2124-3358	10.9°, -45.4°	4.931	250 ± 125	33.6	0.85	—	2.9 ± 0.5	3.4 ± 0.3	1.3 ± 0.2	2.9 ± 0.9	6 ± 6



Spin-down power / distance² (erg/s/kpc²)

